Catalytic kinetics in nanoconfined space of acidic micro/mesoporous materials

Murzin, Dmitry Yu

Published in:
Chemical Engineering Science

DOI:
10.1016/j.ces.2024.120078

Published: 15/07/2024

Document Version
Final published version

Chemical Engineering Science 294 (2024) 120078

Contents lists available at ScienceDirect

Chemical Engineering Science

journal homepage: www.elsevier.com/locate/ces

Catalytic kinetics in nanoconfined space of acidic micro/mesoporous materials

Dmitry Yu. Murzin

Åbo Akademi University, Henriksgatan 2, 20500 Åbo/Turku, Finland

ARTICLE INFO

Keywords:
Zeolites
Two-step sequence
Kinetics
Mesoporosity
Shape-selectivity

ABSTRACT

Kinetics of heterogeneous acid catalyzed reactions is considered for micro-mesoporous materials taking into account nonuniformity of active sites, located in different pores. The methodology for deriving rate equations is developed accounting for reactions in single site nanopores, in macropores/external surfaces of crystals, in narrow nanopores with Gemini sites, as well as in more wider nanoconfined pores with limited pore occupancy. Contribution of such nanoconfined pores was considered using the acid site density as a kinetic descriptor for activity and selectivity. The rate equation was derived for a mechanism with two kinetically significant steps, assuming that the the intermediate size pores accommodate only two molecules. The kinetic treatment accounts for different reactivity of acid sites and lateral interactions.

Modification of zeolites to form mesopores was discussed from the kinetic viewpoint highlighting how such treatment influences activity and selectivity.

Finally, the reactant and product shape selectivity is discussed in a quantitative way.

1. Introduction

Catalysis by solid Brønsted acid catalysts, such as zeolites, is widely spread in oil refining and manufacturing of basic chemicals (Cejka et al., 2010; Jess and Wasserschied, 2013; Murzin, 2022d). The pore structure and morphology along with acidity, acid strength and distribution of acid sites have been used along the years to explain reactivity of catalysts in numerous reactions (Corma et al., 2018; Dib et al., 2021; Li et al., 2021; Zhang et al., 2020).

Complexity of zeolites, comprising pores of different sizes, is not typically reflected in the kinetic analysis of catalytic reactions over zeolites. The acid sites are often considered as isolated and noninteracting with each other, allowing to use classical approaches of heterogeneous catalytic kinetics (Fogler, 2016; Laidler, 1987, Masel, 2011).

On the other hand, presence of active sites with different acid strength (Boronat and Corma, 2019; Derouane et al., 2013; Kubicka et al., 2006), dependence of the rates on the crystal size of zeolite (Damjanovic and Auroux, 2008), pore structure (Arsenova-Härtel et al., 2000) and the acid site density (Barakov et al., 2022; Milakovic et al., 2021; Qi et al., 2016) call for developing the kinetic models, where such phenomena would be explicitly taken into account.

In a simple case of single isolated acid sites, when the active site density, variations in acid strength and confinement in the pores do not influence heterogeneous catalytic reactions, the reaction kinetics with just one adsorbed species per acid site can be described in the same way in a classical Langmuir approach. In such case probabilities of a particular site to be either free or occupied should be used instead of coverage applied in conventional analysis.

For isomerization reaction A ↔ C the following mechanism can be considered.

$$\begin{aligned} &1.\ * + A \leftrightarrow *A \\ &\underline{2.\ *A \leftrightarrow *+C} \\ &A \leftrightarrow C \end{aligned} \quad (1)$$

where * is the acid site, *A,* and *C* are reactants. The rate expression is the same for Eq. (1) as for the two-step sequence (Temkin, 1979).

The approach of Langmuir developed for metal films (Langmuir, 1922) was based on application of the mass action law considering fast diffusion and coverages as a representation of surface concentrations on ideal surfaces. For catalysis on isolated acid sites, similar to catalytic reactions on single atom or single atom alloy (SAA) catalysts (Murzin, 2023), a probability of a site being occupied corresponds to the coverage.

A more complicated case is the situation when there are few (i.e. two) sites inside a pore. These acid sites within a pore can interact with each other, which is reflected in different values of the rate constants

E-mail address: dmurzin@abo.fi.

https://doi.org/10.1016/j.ces.2024.120078
Received 10 January 2024; Received in revised form 19 March 2024; Accepted 31 March 2024
Available online 5 April 2024

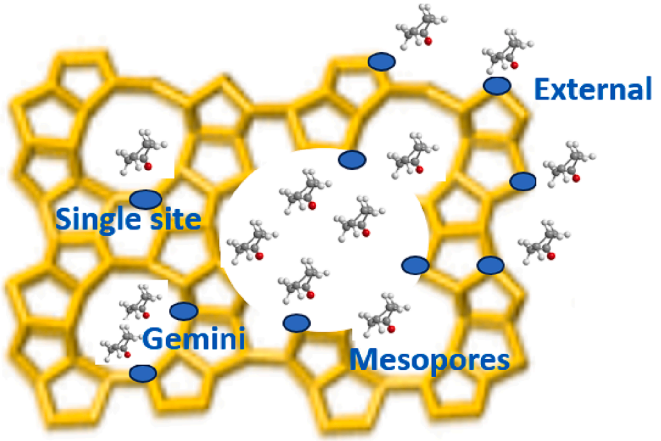

Fig. 1. A simplified cartoon of the acid sites in zeolites.

compared to an isolated site. Molecules adsorbed on such sites can be exposed to lateral interactions, which are dependent on the proximity of sites, i.e. acid site density (Fig. 1).

Moreover, zeolites, being microporous materials, also contain acid sites on the external surface.

Turnover frequency (TOF) calculated per proton can be thus dependent of the acid site density (Barakov et al., 2022; Laluc et al., 2021; Milakovic et al., 2021), even passing through a maximum. A mechanistic framework was recently developed (Murzin, 2022a), accounting for such dependencies not only for activity /TOF, but also selectivity.

In the current treatment, the intention is to combine catalytic kinetics on zeolitic materials, which contain all kind of pores with isolated acid sites, a pair of sites and macropores with the acid site density as a descriptor. A special focus will be on the Gemini type of acid sites, i.e. a pair of acid sites in a micropore. Such approach, directly accounting for presence of different types of sites in a zeolitic material with nano- and mesopores, is not discussed in the literature, highlighting the novelty of the current kinetic treatment.

2. Counting sites: Isolated sites, mesopores and outer crystal surfaces

For isolated sites the approach is similar to a classical approach of catalytic kinetics where instead of a surface coverage a probability of a site to be free or occupied should be used.

For catalysis in mesopores with nanoconfinement and interactions between adsorbed molecules in the current treatment it is assumed that only two catalytically active acid sites are in close proximity leading to a situation when one molecule of the reactant can be adsorbed on one site and another one on the neighboring site. Such considerations are similar to cooperative kinetics previously discussed for catalysis on metal nanoclusters with two (Murzin, 2022b) or even more available sites (Murzin, 2022c). In general, not only real mesoporosity of the type discussed above can be present in micro-mesoporous materials, but also mesoporosity related to interparticle voids. In the context of the kinetic treatment in the current work, the corresponding acid sites are considered as the sites on the external surface of particles.

For a two-step sequence with several sites the reaction mechanism can be expressed through reactions on single sites, Gemini type of sites in narrow pores with just two sites, which proximity of the acid sites imposes their mutual influence, in wider mesopores, where the rate depends on acid site density and finally on the outer surface of zeolites crystals.

1'.* +A↔I* +C	0	1	0	0	0
2'. I*+B↔*+D	0	1	0	0	0
1''.I* +A↔II* +C	0	0	1	0	0
2''. II*+B↔I*+D	0	0	1	0	0
1'''* +A↔I* +C	0	0	0	1	0
2'''. I*+B↔I+D	0	0	0	1	0
1''''* +A↔I* +C	0	0	0	0	1
2''''. I*+B↔I+D	0	0	0	0	1

$N^{(S)}$, $N^{(G')}$, $N^{(G'')}$, $N^{(M)}$, $N^{(C)}$: A+B ↔ C+D (2)

In Eq. (2) the numbers (0 or 1) correspond to the stoichiometric numbers (i.e. Horiuti numbers) of a particular step in the corresponding reaction route (Horiuti and Nakamura, 1967; Murzin and Salmi, 2016; Temkin, 1979).

The first reaction route $N^{(S)}$ corresponds to the catalytic reaction on single sites inside the zeolite pores. The last route reflects reactions on the outer surface of zeolite crystals giving the classical kinetic expression of the two-step sequence. The route $N^{(G')}$ reflects the reaction on a bare site of the Gemini pair. In a general case when some interactions between the adjacent Gemini sites are present, the rate constants on this bare site are different from the rate constants along the first reaction route $N^{(S)}$. The route $N^{(G'')}$ corresponds to the reaction on the second Gemini site inside a mesopore when the first one is occupied by the intermediate I. Finally, the route $N^{(M)}$ reflects reactions in nanoconfined space which kinetics is dependent on the acid site density (Murzin, 2022a).

For the derivation of kinetic equations, it will be considered that the overall number of catalytically active sites N is equal to the sum of singles sites N_S, Gemini pairs N_G and sites on the outer surface of the zeolite crystals

$$N = N_S + N_G + N_M + N_C \tag{3}$$

Eq. (3) does not distinguish between the Lewis and Brønsted acid sites, which should be considered in a general case. The derivation below will thus take into account first only one type of sites and then will be extended to the sites of different nature. It is well known (Cejka et al., 2010), that zeolites exhibit a distribution of sites with different acid strength. In the current work such variability of sites is considered explicitly by using different kinetic constants for reactions occurring on different types of sites (i.e. single sites in narrow pores, Gemini sites in narrow mesopores, sites in wider mesopores and finally acid sites in large mesopores/outer crystal surfaces).

For the single sites the steady state approximation is valid for the reaction route $N^{(S)}$

$$r_{+1} - r_{-1} = r_{+2} - r_{-2} \tag{4}$$

It can be written in a form, which includes the amount of bare $N_{0,s}$ and occupied single sites $N_{1,s}$

$$k_{+1,s}C_A N_{0,s} - k_{-1,s}C_C N_{1,s} = k_{+2,s}C_B N_{1,s} - k_{-2,s}C_D N_{0,s} \tag{5}$$

The concentration of the acid sites free from adsorbed species can be obtained from the site balance

$$N_{0,s} + N_{1,s} = N_S \tag{6}$$

Derivation of the rate expression for the two-step sequencies was treated in the textbooks and monographs (Murzin and Salmi, 2016; Temkin, 1979), therefore only the final rate expression for the reversible reaction is presented below

$$r^{(S)} = r_s N_S = \frac{(\omega^s_{+1}\omega^s_{+2} - \omega^s_{-1}\omega^s_{-2})N_S}{\omega^s_{+1} + \omega^s_{+2} + \omega^s_{-1} + \omega^s_{-2}} \tag{7}$$

Where $r^{(S)}$ is the rate along a route, and the reaction rate per site r_s is expressed through frequencies of steps, e.g. $\omega^s{}_{+1} = k_{+1,s}C_A$, $\omega^s{}_{-1} = k_{-1,s}C_C$.

For the reactions on Gemini pairs the steady state approximation for

both reaction routes takes the form

$$k_{+1,G}C_A N_{0,G} - k_{-1,G}C_C N_{1,G} = k_{+2,G}C_B N_{1,G} - k_{-2,G}C_D N_{0,G} \quad (8)$$

$$k'_{+1,G}C_A N_{1,G} - k'_{-1,G}C_C N_{2,G} = k'_{+2,G}C_B N_{2,G} - k'_{-2,G}C_D N_{1,G} \quad (9)$$

From this the amounts of bare and occupied sites in Gemini pairs are

$$N_{1,G} = U_1 N_{0,G}; N_{2,G} = U_1 U_2 N_{0,G} \quad (10)$$

Where U_1 and U_2 are

$$U_1 = \frac{k_{+1,G}C_A + k_{-2,G}C_D}{k_{+2,G}C_B + k_{-1,G}C_C} = \frac{\omega_{+1}^{G,1} + \omega_{-2}^{G,1}}{\omega_{+2}^{G,1} + \omega_{-1}^{G,1}} \quad (11)$$

$$U_2 = \frac{k'_{+1,G}C_A + k'_{-2,G}C_D}{k'_{+2,G}C_B + k'_{-1,G}C_C} = \frac{\omega_{+1}^{G,2} + \omega_{-2}^{G,2}}{\omega_{+2}^{G,2} + \omega_{-1}^{G,2}} \quad (12)$$

Obviously the superscript ^{G,1} corresponds to the rate constants for the first site in the Gemini pair when the second is bare, while the superscript ^{G,2} reflects the situation of a reaction on a second site, when the first one is occupied.

The mass balance for the Gemini pairs is

$$N_{0,G} + N_{1,G} + N_{2,G} = N_G \quad (13)$$

giving an expression for the bare sites in the Gemini pair

$$N_{0,G} = \frac{N_G}{1 + U_1 + U_1 U_2} \quad (14)$$

For the reaction on the Gemini sites the reaction rate along two routes $N^{(G')}$ and $N^{(G'')}$ is

$$r^{(G')} + r^{(G')} = r'_{+1} - r'_{-1} + r''_{+1} - r''_{-1} =$$

$$= \omega_{+1}^{G,1} N_{o,G} - \omega_{-1}^{G,1} N_{1,G} + \omega_{+1}^{G,2} N_{1,G} - \omega_{-1}^{G,2} N_{2.G} \quad (15)$$

resulting in

$$r^{(G')} + r^{(G')} = \frac{(\omega_{+1}^{G,1} + \omega_{+1}^{G,2} U_1 - \omega_{-1}^{G,1} U_1 - \omega_{-1}^{G,2} U_1 U_2) N_G}{1 + U_1 + U_1 U_2} \quad (16)$$

The rate along the reaction route $N^{(C)}$ can be easily written as it is similar in fact to the reaction route $N^{(S)}$ with just different rate constants

$$r^{(C)} = \frac{(\omega_{+1}^{C}\omega_{+2}^{C} - \omega_{-1}^{C}\omega_{-2}^{C}) N_C}{\omega_{+1}^{C} + \omega_{+2}^{C} + \omega_{-1}^{C} + \omega_{-2}^{C}} \quad (17)$$

In the treatment below it will be considered that the kinetic parameters do not depend on the crystal faces, and the acid sites exhibit the same reactivity. A more general treatment could consider the crystal size dependence of a particular reaction, implying that different crystallographic faces on the external surface of a zeolite display different reactivity.

The reaction rates for the nanoconfined spaces were considered by Murzin (2022a) using the acid site density as a descriptor. Such approach simplifies derivation of the rate equations for sites of different reactivity. Instead of explicitly accounting for different rate constants for transformations of several molecules within a nanoconfined space, the variations of the rate constants within a pore are linked to the electrostatic contribution to the Gibbs energy of the solid surface with acid sites:

$$\Delta G_{es} = \frac{N_A Z_{H^+} Z_{H^+} e^2}{4\pi\varepsilon_0 \varepsilon d_{ave,H^+-H^+}} = \frac{\varphi Z_{H^+} Z_{H^+}}{d_{ave,H^+-H^+}} \quad (18)$$

where Z_{H^+} is the charge of acid sites/hydronium ions, d_{ave,H^+-H^+} is the average distance between these ions/acid sites, ε_0 is the permittivity in vacuum, ε dielectric constant, e is the charge of the electron, N_A is the Avogadro's number, and φ is the lumped constant $\varphi = N_A e^2/4\pi\varepsilon_0\varepsilon$. For adsorption on the acid sites (Murzin, 2022a) with a partial donation of protons to the adsorbate the Gibbs energy of adsorption on the acid sites it was suggested that changes in the electrostatic contribution are expressed as

$$\Delta G_{ads} = \Delta G^0_{ads,nes} + \delta_{Z_{H^+}} \frac{\varphi}{d_{ave,H^+-H^+}} \quad (19)$$

where $\delta_{Z_{H^+}}$ is the increment of the electrostatic contribution to the Gibbs energy upon adsorption on the acid sites.

The average distance between the acid sites can be calculated through the density of acid sites ρ_{H^+} (mol/g) defined via the surface area of mesopores divided by the effective area around the surface site, in the simplest case calculated as a circle with the diameter equal to the average distance between acid sites

$$\rho_{H^+} = \frac{S_{N_2,mesopores}}{\frac{\pi d^2_{ave,H^+-H^+}}{4} N_A} \quad (20)$$

The rate constants for the two-step sequence depending on the acid site density were discussed by Murzin (2022a) giving

$$k_{+1_{(H^+)}} = k_{+1} e^{-\alpha_1 \varphi' \sqrt{\rho_{H^+}}}, k_{-1_{(H^+)}} = k_{-1} e^{(1-\alpha_1)\varphi' \sqrt{\rho_{H^+}}}, k_{+2_{(H^+)}}$$
$$= k_{+2} e^{(1-\alpha_2)\varphi' \sqrt{\rho_{H^+}}}, k_{-2_{(H^+)}} = k_{-2} e^{-\alpha_2 \varphi' \sqrt{\rho_{H^+}}}, \quad (21)$$

Where α_1 and α_2 are the Polanyi parameters of the first step and second steps and

$$\varphi' = \frac{\delta_{Z_{H^+}} N_A e^2}{4\pi\varepsilon_0 \varepsilon} \sqrt{\frac{\pi N_A}{4 S_{N_2,mesopores}}} \quad (22)$$

Eq. (22) is different from the previous considerations in (Murzin, 2022a) as in the current treatment the surface area of mesopores is explicitly considered. Considering the general form of the two-step sequence and the rate constant dependence on the acid site density, an expression for the reaction rate along the route $N^{(M)}$ is

$$r^{(M)} = \frac{(\omega_{+1}^{M}\omega_{+2}^{M} - \omega_{-1}^{M}\omega_{-2}^{M}) e^{(1-\alpha_2-\alpha_1)\varphi' \sqrt{\rho_{H^+}}} N_M}{\omega_{+1}^{M} e^{-\alpha_1 \varphi' \sqrt{\rho_{H^+}}} + \omega_{+2}^{M} e^{(1-\alpha_2)\varphi' \sqrt{\rho_{H^+}}} + \omega_{-1}^{M} e^{(1-\alpha_1)\varphi' \sqrt{\rho_{H^+}}} + \omega_{-2}^{M} e^{-\alpha_2 \varphi' \sqrt{\rho_{H^+}}}} \quad (23)$$

Where ω_{+1}^{M}, etc. are acid site density independent frequencies of steps

The overall rate along four routes can be thus expressed

$$r = \frac{(\omega_{+1}^{s}\omega_{+2}^{s} - \omega_{-1}^{s}\omega_{-2}^{s})}{\omega_{+1}^{s} + \omega_{+2}^{s} + \omega_{-1}^{s} + \omega_{-2}^{s}} N_S + \frac{\left(\omega_{+1}^{G,1}\omega_{+2}^{G,1} - \omega_{-1}^{0}\omega_{-2}^{0} + \left(\omega_{+1}^{G,2}\omega_{+2}^{G,2} - \omega_{-1}^{G,2}\omega_{-2}^{G,2}\right)\frac{\omega_{+1}^{G,1} + \omega_{-2}^{G,1}}{\omega_{+2}^{G,2} + \omega_{-1}^{G,2}}\right)}{\omega_{+1}^{G,1} + \omega_{+2}^{G,1} + \omega_{-1}^{G,1} + \omega_{-2}^{G,1} + \left(\omega_{+1}^{G,1} + \omega_{-2}^{G,1}\right)\frac{\omega_{+1}^{G,2} + \omega_{-2}^{G,2}}{\omega_{+2}^{G,2} + \omega_{-1}^{G,2}}} N_G$$
$$+ \frac{(\omega_{+1}^{M}\omega_{+2}^{M} - \omega_{-1}^{M}\omega_{-2}^{M}) e^{(1-\alpha_2-\alpha_1)\varphi' \sqrt{\rho_{H^+}}} N_M}{\omega_{+1}^{M} e^{-\alpha_1 \varphi' \sqrt{\rho_{H^+}}} + \omega_{+2}^{M} e^{(1-\alpha_2)\varphi' \sqrt{\rho_{H^+}}} + \omega_{-1}^{M} e^{(1-\alpha_1)\varphi' \sqrt{\rho_{H^+}}} + \omega_{-2}^{M} e^{-\alpha_2 \varphi' \sqrt{\rho_{H^+}}}} + \frac{(\omega_{+1}^{C}\omega_{+2}^{C} - \omega_{-1}^{C}\omega_{-2}^{C}) N_C}{\omega_{+1}^{C} + \omega_{+2}^{C} + \omega_{-1}^{C} + \omega_{-2}^{C}} \quad (24)$$

Eq. (24) contains thus in an explicit way contributions of different types of sites to the overall reaction rate. In fact, within a narrow mesopore, not only two sites are possible. A general case of n-molecules adsorbed in nanoconfined space was considered in (Murzin, 2022c) and can be presented as

$$r_{NM} = \left(\frac{\left(\omega^{I}_{+1} + \omega^{II}_{+1}U_1 + \omega^{III}_{+1}U_1U_2 + .. + \omega^{n}_{+1}U_1U_2..U_{n-1}\right)}{1 + U_1 + U_1U_2 + U_1U_2U_3 + ... + U_1U_2U_3...U_n} - \frac{\left(\omega^{I}_{-1}U_1 + \omega^{II}_{-1}U_1U_2 + \omega^{III}_{-1}U_1U_2U_3 + .. + \omega^{n}_{-1}U_1U_2..U_n\right)}{1 + U_1 + U_1U_2 + U_1U_2U_3 + ... + U_1U_2U_3...U_n}\right)N_{NM} \tag{25}$$

Where r_{NM} and N_{NM} correspond to the reaction rate and the number of acid sites in narrow mesopores. For the arbitrary route J with the corresponding number of *j* species in a pore it holds

$$U_j = \frac{\omega^{J}_{+1} + \omega^{J}_{-2}}{\omega^{J}_{+2} + \omega^{J}_{-1}} \tag{26}$$

Apparently, the number of adsorbed species in a pore depends on the size of the pore and the size of the reacting molecule. It can be assumed that in nanoconfined space the total number of adsorbed reactants in a pore n is related to the pore volume, the molecular volume and the parameter ϕ reflecting the geometrical/shielding constraints. The latter parameter appears due to steric constrains and a mismatch in the size of molecules and the pore volume leading to only partial occupancy of acid sites inside the pore compared to the maximum possible:

$$n = n_{max}\phi = \frac{V_{adsorbed\_species}}{V_{pore}}\phi \tag{27}$$

In catalysis by zeolites/mesoporous materials contribution of both Lewis and Brønsted acid sites should be taken into account for a particular zeolite resulting in a general expression

$$r = r^{B}_{S}N^{B}_{S} + r^{L}_{S}N^{L}_{S} + r^{B}_{NM}N^{B}_{NM} + r^{L}_{NM}N^{L}_{NM} + r^{B}_{M}N^{B}_{M} + r^{L}_{M}N^{L}_{M} + r^{B}_{C}N^{B}_{C} + r^{L}_{C}N^{L}_{C} \tag{28}$$

Obviously, the number of Lewis and Brønsted acid is different depending on the material, and in some cases for example a certain type of acid site might be absent. For example, Lewis acid sites are typically associated with Al^{3+}, however, other T (tetrahydra) ions have been introduced into zeolitic materials, including Ga^{3+}, Fe^{3+} or B^{3+} with a charge mismatch and thus presence of Brønsted acid sites to compensate the charge (Suib et al., 2023). Subsequently eq. (28) in such a case contains not one type of Lewis acid sites for each subset of active sites. Moreover, besides trivalent cations, tetravalent counterparts (e.g. Ti^{4+}, Ge^{4+}, Sn^{4+}, Zr^{4+}, Hf^{4+}) have been extensively investigated, resulting in formation of Lewis acid sites of another type than Al^{3+}(Suib et al., 2023). Such sites with other values of kinetic parameters should be apparently distinguished from classical Lewis acid sites and a result additional terms accounting for such sites should be introduced in eq. (28).

Alternatively, for the materials such as layered zeolites (Shamzhy et al., 2021), when the reactions proceed almost exclusively on the external surfaces of zeolites, the terms accounting for reactions in nanopores would vanish.

3. Catalysis in micropores

3.1. Reaction rates on single sites and in narrow mesopores

For the illustration purposes analysis of eq. (28) will be done for irreversible reactions considering the second step in the two- step sequence as equal to zero. For the reaction occurring only in micropores with a single site and narrow mesopores with maximum two reacting molecules on Brønsted acid sites $N_{S,B}$ and $N_{NM,B}$ respectively, the rate expression takes the form

$$r = r^{B}_{s}N^{B}_{s} + r^{B}_{s}N^{B}_{NM} = \frac{\left(\omega^{s}_{+1}\omega^{s}_{+2}\right)}{\omega^{s}_{+1} + \omega^{s}_{+2} + \omega^{s}_{-1}}N^{B}_{s} + \frac{\left(\omega^{G,1}_{+1}\omega^{G,1}_{+2} + \omega^{G,2}_{+1}\omega^{G,2}_{+2}\frac{\omega^{G,1}_{+1}}{\omega^{G,2}_{+2}+\omega^{G,2}_{-1}}\right)}{\omega^{G,1}_{+1} + \omega^{G,1}_{+2} + \omega^{G,1}_{-1} + \left(\omega^{G,1}_{+1}\right)\frac{\omega^{G,2}_{+1}}{\omega^{G,2}_{+2}+\omega^{G,2}_{-1}}}N^{B}_{NM} \tag{29}$$

The reaction scheme in eq. (2) and thus eq. (29) can be further simplified by assuming that the concentration of the reactant B is an excess, not changing with time. This leads to the rate expression, where the apparent constants, e.g. k^{s}_{+2}, *app*, contain the concentration of that reactant

$$r = \frac{\left(k^{s}_{+1}k^{s}_{+2,app}C_A\right)}{k^{s}_{+1}C_A + k^{s}_{+2,app} + k^{s}_{-1}C_C}N^{B}_{s} + \frac{\left(k^{G,1}_{+1}k^{G,1}_{+2,app}C_A + \frac{k^{G,1}_{+1}k^{G,2}_{+1}k^{G,2}_{+2,app}C^{2}_{A}}{k^{G,2}_{+2,app}+k^{G,2}_{-1}C_C}\right)}{k^{G,1}_{+1}C_A + k^{G,1}_{+2,app} + k^{G,1}_{-1}C_C + \frac{k^{G,1}_{+1}k^{G,2}_{+1}C^{2}_{A}}{k^{G,2}_{+2,app}+k^{G,2}_{-1}C_C}}N^{B}_{NM} \tag{30}$$

The left-hand side of Eq. (30) resembles the well-known expression for the two-step sequence with one irreversible step and can be rewritten in the form of the Michaelis-Menten equation for enzymatic catalysis or its Eley-Rideal equivalent in heterogeneous catalytic kinetics. The right hand-side is a simplified version of kinetics with allosteric enzymes when the rate can increase with the concentration elevation giving the reaction order exceeding unity (Murzin and Salmi, 2016). Clearly, at high substrate concentrations the maximum of the rate is obtained.

To elucidate the influence of catalysis in narrow macropores with two acid sites the reaction rate for such case r_{s+nm} can be compared with the rate only on single sites assuming that the number of single sites does not depend on the presence of narrow mesopores

$$\frac{r_{s+nm}}{r_s} = \frac{\frac{\left(k^{s}_{+1}k^{s}_{+2,app}C_A\right)}{k^{s}_{+1}C_A+k^{s}_{+2,app}+k^{s}_{-1}C_C}N^{B}_{s} + \frac{\left(k^{G,1}_{+1}k^{G,1}_{+2,app}C_A+\frac{k^{G,1}_{+1}k^{G,2}_{+1}k^{G,2}_{+2,app}C^{2}_{A}}{k^{G,2}_{+2,app}+k^{G,2}_{-1}C_C}\right)}{k^{G,1}_{+1}C_A+k^{G,1}_{+2,app}+k^{G,1}_{-1}C_C+\frac{k^{G,1}_{+1}k^{G,2}_{+1}C^{2}_{A}}{k^{G,2}_{+2,app}+k^{G,2}_{-1}C_C}}N^{B}_{NM}}{\frac{\left(k^{s}_{+1}k^{s}_{+2,app}C_A\right)}{k^{s}_{+1}C_A+k^{s}_{+2,app}+k^{s}_{-1}C_C}N^{B}_{s}} = 1 + \frac{\left(k^{G,1}_{+1}k^{G,1}_{+2,app}C_A + \frac{k^{G,1}_{+1}k^{G,2}_{+1}k^{G,2}_{+2,app}C^{2}_{A}}{k^{G,2}_{+2,app}+k^{G,2}_{-1}C_C}\right)\left(k^{s}_{+1}C_A + k^{s}_{+2,app} + k^{s}_{-1}C_C\right)}{\left(k^{G,1}_{+1}C_A + k^{G,1}_{+2,app} + k^{G,1}_{-1}C_C + \frac{k^{G,1}_{+1}k^{G,2}_{+1}C^{2}_{A}}{k^{G,2}_{+2,app}+k^{G,2}_{-1}C_C}\right)\left(k^{s}_{+1}k^{s}_{+2,app}C_A\right)}\frac{N^{B}_{NM}}{N^{B}_{s}} \tag{31}$$

In a more general case, when for example mesoporosity is created by dealumination or desilication the number of single sites after such treatment is apparently different and should be explicitly taken into account

$$\frac{r_{s+nm}}{r_s} = \frac{N^{B}_{s,aftertreatment}}{N^{B}_{s,priortreatment}}\frac{\left(k^{G,1}_{+1}k^{G,1}_{+2,app}C_A + \frac{k^{G,1}_{+1}k^{G,2}_{+1}k^{G,2}_{+2,app}C^{2}_{A}}{k^{G,2}_{+2,app}+k^{G,2}_{-1}C_C}\right)\left(k^{s}_{+1}C_A + k^{s}_{+2,app} + k^{s}_{-1}C_C\right)}{\left(k^{G,1}_{+1}C_A + k^{G,1}_{+2,app} + k^{G,1}_{-1}C_C + \frac{k^{G,1}_{+1}k^{G,2}_{+1}C^{2}_{A}}{k^{G,2}_{+2,app}+k^{G,2}_{-1}C_C}\right)\left(k^{s}_{+1}k^{s}_{+2,app}C_A\right)}\frac{N^{B}_{NM,aftertreatment}}{N^{B}_{s,priortreatment}} \tag{32}$$

The ratio of rates obviously depends on the absolute values of rate constants for the single acid sites and narrow mesopores with two (Gemini) sites. In the case of Eley-Rideal mechanism (first step at equilibrium) eq. (32) can be written as

$$\frac{r_{s+nm}}{r_s}=\frac{N^B_{s,aftertreatment}}{N^B_{s,priortreatment}}\frac{\left(K_1^{G,1}k_{+2,app}^{G,1}C_A+K_1^{G,1}k_{+2,app}^{G,2}\left(K_1^{G,2}\right)^2C_A^2/C_C\right)\left(K_1^SC_A+C_C\right)}{\left(C_C+K_1^{G,1}C_A+K_1^{G,1}K_1^{G,2}C_A^2/C_C\right)k_{+2,app}^sK_1^SC_A}\frac{N^B_{NM,aftertreatment}}{N^B_{s,priortreatment}} \tag{33}$$

For the isomerization reaction A->D, eq. (33) can be further simplified

$$\frac{r_{s+nm}}{r_s}=\frac{N^B_{s,aftertreatment}}{N^B_{s,priortreatment}}\frac{\left(K_1^{G,1}k_{+2}^{G,1}C_A+K_1^{G,1}k_{+2}^{G,2}\left(K_1^{G,2}\right)^2C_A^2\right)\left(K_1^SC_A+1\right)}{\left(1+K_1^{G,1}C_A+K_1^{G,1}K_1^{G,2}C_A^2\right)k_{+2}^sK_1^SC_A}\frac{N^B_{NM,aftertreatment}}{N^B_{s,priortreatment}} \tag{34}$$

If adsorption on the first site of a Gemini pair is independent on the presence of the second site in its vicinity, the rate parameters for such case are the same as for the single site, giving a simplified version of Eq. (34)

$$\frac{r_{s+nm}}{r_s}=\frac{N^B_{s,aftertreatment}}{N^B_{s,priortreatment}}+\frac{\left(K_1^Sk_{+2}^sC_A+K_1^sk_{+2}^{G,2}\left(K_1^{G,2}\right)^2C_A^2\right)\left(K_1^SC_A+1\right)}{\left(1+K_1^SC_A+K_1^SK_1^{G,2}C_A^2\right)k_{+2}^sK_1^SC_A}\frac{N^B_{NM,aftertreatment}}{N^B_{s,priortreatment}} \tag{35}$$

Even for this simplified case different options of the rate enhancement or deterioration are possible. This depends on the number of acid sites generated after creation of mesoprosity as well as on the changes in the rate and adsorption constants for the reaction on the second site of the Gemini pair when the first site is occupied

$$\frac{r_{s+nm}}{r_s}=\frac{N^B_{s,aftertreatment}}{N^B_{s,priortreatment}}+\frac{k_{+2}^sK_1^SC_A+\left(k_{+2}^s\left(K_1^s\right)^2+K_1^sk_{+2}^{G,2}\left(K_1^{G,2}\right)^2\right)C_A^2+k_{+2}^{G,2}\left(K_1^s\right)^2\left(K_1^{G,2}\right)^2C_A^3}{k_{+2}^sK_1^SC_A+k_{+2}^s\left(K_1^s\right)^2C_A)^2+k_{+2}^s\left(K_1^s\right)^2K_1^{G,2}C_A^3}\frac{N^B_{NM,aftertreatment}}{N^B_{s,priortreatment}} \tag{36}$$

Obviously, the ratio of rates depends on how many sites are created after the treatment leading to some mesoporosity and also on the rate parameters on the second site $k_{+2}^{G,2}$ and $K_1^{G,2}$. Large attractive interactions elevating these values will lead to the rate enhancement. On the contrary for repulsive interactions and significant rate retardation on the second site of the Gemini pair eq. (35) gives as expected only dependence on the number of sites

$$\frac{r_{s+nm}}{r_s}=\frac{N^B_{s,\ after\ treatment}}{N^B_{s,\ prior\ treatment}}+\frac{N^B_{NM,\ after\ treatment}}{N^B_{s,\ prior\ treatment}} \tag{37}$$

3.2. Reaction orders

For the reaction A->D the reaction rate on single sites is

$$r=\frac{\left(k_{+1}^sk_{+2}^sC_A\right)}{k_{+1}^sC_A+k_{+2}^s+k_{-1}^s}N_s^B \tag{38}$$

The apparent reaction order is defined as

$$n_{A,app}=\frac{\partial lnr}{\partial lnC_A} \tag{39}$$

For the reactions on the single sites it is

$$n^s_{A,app}=\frac{\partial ln(k_{+1}^sk_{+2}^sC_A)N_s^B}{\partial lnC_A}-\frac{\partial ln(k_{+1}^sC_A+k_{+2}^s+k_{-1}^s)}{\partial lnC_A} \tag{40}$$

which after some transformations results in the apparent reaction order for the reaction on single sites

$$n^s_{A,app}=1-\frac{\partial ln\left(C_A+\frac{k_{+2}^s+k_{-1}^s}{k_{+1}^s}\right)}{\partial lnC_A}=1-C_A\frac{\frac{\partial\left(C_A+\frac{k_{+2}^s+k_{-1}^s}{k_{+1}^s}\right)}{\partial C_A}}{C_A+\frac{k_{+2}^s+k_{-1}^s}{k_{+1}^s}}=$$

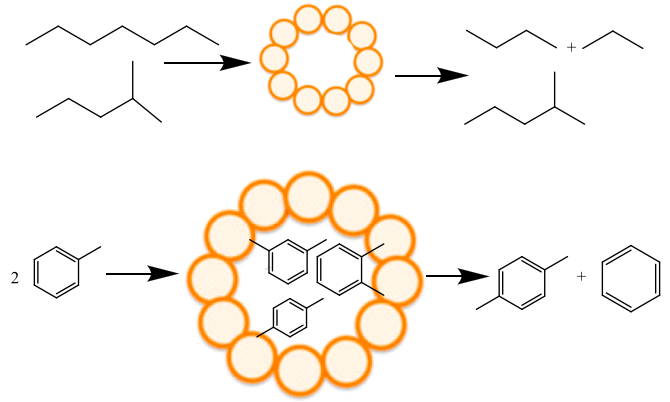

Fig. 2. Shape selectivity in catalysis by zeolites.

$$= 1 - \frac{C_A}{C_A + \frac{k^s_{+2}+k^s_{-1}}{k^s_{+1}}} = \frac{\frac{k^s_{+2}+k^s_{-1}}{k^s_{+1}}}{C_A + \frac{k^s_{+2}+k^s_{-1}}{k^s_{+1}}} = \frac{1}{\frac{k^s_{+1}C_A}{k^s_{+2}+k^s_{-1}} + 1} \tag{41}$$

The reaction order in the substrate thus depends on the substrate concentration being equal to one at low values and reaching the zero order at high substrate concentration when $\frac{k^s_{+1}C_A}{k^s_{+2}+k^s_{-1}}$ substantially exceeds unity.

For the reaction on the Gemini pairs with the rate expression

$$r = \frac{\left(k^{G,1}_{+1}k^{G,1}_{+2,}C_A + \frac{k^{G,1}_{+1}k^{G,2}_{+1}k^{G,2}_{+2}C_A^2}{k^{G,2}_{+2,app}+k^{G,2}_{-1}}\right)}{k^{G,1}_{+1}C_A + k^{G,1}_{+2} + k^{G,1}_{-1} + \frac{k^{G,1}_{+1}k^{G,2}_{+1}C_A^2}{k^{G,2}_{+2}+k^{G,2}_{-1}}} N^B_G \tag{42}$$

The apparent reaction order is

$$n^G_{A,app} = \frac{\partial ln C_A (k^{G,1}_{+2} + \frac{k^{G,2}_{+1}k^{G,2}_{+2}}{k^{G,2}_{+2,app}+k^{G,2}_{-1}}C_A)}{\partial ln C_A} - \frac{\partial ln (C_A + \frac{k^{G,1}_{+2}+k^{G,1}_{-1}}{k^{G,1}_{+1}} + \frac{k^{G,2}_{+1}C_A^2}{k^{G,2}_{+2}+k^{G,2}_{-1}})}{\partial ln C_A} \tag{43}$$

and

$$n^G_{A,app} = 1 + C_A \frac{\frac{\partial (k^{G,1}_{+2} + C_A \frac{k^{G,2}_{+1}k^{G,2}_{+2}}{k^{G,2}_{+2,app}+k^{G,2}_{-1}})}{\partial C_A}}{k^{G,1}_{+2} + C_A \frac{k^{G,2}_{+1}k^{G,2}_{+2}}{k^{G,2}_{+2,app}+k^{G,2}_{-1}}} - C_A \frac{\frac{\partial (C_A + \frac{k^{G,1}_{+2}+k^{G,1}_{-1}}{k^{G,1}_{+1}} + \frac{k^{G,2}_{+1}C_A^2}{k^{G,2}_{+2}+k^{G,2}_{-1}})}{\partial C_A}}{C_A + \frac{k^{G,1}_{+2}+k^{G,1}_{-1}}{k^{G,1}_{+1}} + \frac{k^{G,2}_{+1}C_A^2}{k^{G,2}_{+2}+k^{G,2}_{-1}}} =$$

$$= 1 + \frac{\frac{k^{G,2}_{+1}k^{G,2}_{+2}}{k^{G,2}_{+2,app}+k^{G,2}_{-1}}C_A}{k^{G,1}_{+2} + C_A \frac{k^{G,2}_{+1}k^{G,2}_{+2}}{k^{G,2}_{+2,app}+k^{G,2}_{-1}}} \frac{C_A + 2\frac{k^{G,2}_{+1}C_A^2}{k^{G,2}_{+2}+k^{G,2}_{-1}}}{C_A + \frac{k^{G,1}_{+2}+k^{G,1}_{-1}}{k^{G,1}_{+1}} + \frac{k^{G,2}_{+1}C_A^2}{k^{G,2}_{+2}+k^{G,2}_{-1}}} + \frac{\frac{k^{G,2}_{+1}k^{G,2}_{+2}}{k^{G,2}_{+2,app}+k^{G,2}_{-1}}C_A}{k^{G,1}_{max} + C_A \frac{k^{G,2}_{+1}k^{G,2}_{+2}}{k^{G,2}_{+2,app}+k^{G,2}_{-1}}}$$

$$+ \frac{\frac{k^{G,1}_{+2}+k^{G,1}_{-1}}{k^{G,1}_{+1}} - \frac{k^{G,2}_{+1}C_A^2}{k^{G,2}_{+2}+k^{G,2}_{-1}}}{C_A + \frac{k^{G,1}_{+2}+k^{G,1}_{-1}}{k^{G,1}_{+1}} + \frac{k^{G,2}_{+1}C_A^2}{k^{G,2}_{+2}+k^{G,2}_{-1}}} \tag{44}$$

Apparently according to eq. (43) the reaction order in the substrate can exhibit a rather rich behavior, especially compared to the reaction on single sites.

It is apparently clear from eq. (41) that depending on the values of the rate and adsorption constants, different behavior can be expected for the forward rate including the second order in the reactant *A* or even a maximum in the rate upon an increase in the reactant *A* concentration. The latter case is possible if the transformation rate of A to D is diminished due to the lateral interactions between two molecules of *A* within the pore. A similar situation with the corresponding numerical simulations was discussed for the case of adsorption in the nanoconfined space on nanoclusters (Murzin, 2022b, 2022c) demonstrating the rate maxima for the forward reaction for the conventional Eley-Rideal mechanism, which should not give any maxima in the conventional kinetic treatment.

3.3. Creation of mesoporosity in micropores materials

Extension beyond two Brønsted sites considering explicitly the number of molecules results for the overall irreversible case

$$r_{s+nm} = \frac{(\omega^s_{+1}\omega^s_{+2})}{\omega^s_{+1} + \omega^s_{+2} + \omega^s_{-1}} N^B_s + \frac{(\omega^I_{+1} + \omega^{II}_{+1}U_1 + \omega^{III}_{+1}U_1U_2 + .. + \omega^n_{+1}U_1U_2..U_{n-1})}{1 + U_1 + U_1U_2 + U_1U_2U_3 + ... + U_1U_2U_3...U_n} N^B_{NM} \tag{45}$$

and subsequently the ratio between the rates for zeolites with narrow mesopores to the rate for materials with only single isolated sites takes the form

$$\frac{r_{s+nm}}{r_s} = \frac{N^B_{s,aftertreatment}}{N^B_{s,priortreatment}} + \frac{(\omega^I_{+1} + \omega^{II}_{+1}U_1 + \omega^{III}_{+1}U_1U_2 + .. + \omega^n_{+1}U_1U_2..U_{n-1})}{1 + U_1 + U_1U_2 + U_1U_2U_3 + ... + U_1U_2U_3...U_n} \frac{(\omega^s_{+1} + \omega^s_{+2} + \omega^s_{-1})}{\omega^s_{+1}\omega^s_{+2}} \frac{N^B_{NM,aftertreatment}}{N^B_{s,priortreatment}} \tag{46}$$

Rigorous analysis of eq. (45) requires understanding of the rate constants dependence on the number of species already present in a narrow mesopore.

Moreover, the discussion above considered zeolites as rigid structures, which is not necessarily the case (Ghojavand et al., 2023) as zeolites can exhibit certain framework flexibility in the presence of guest molecules. Such flexibility is manifested in a larger number of adsorbed molecules per unit cell than anticipated from purely geometric considerations. The adsorption behavior of the guest molecules is featured by an inflection point (S-shape behavior) in the adsorption isotherms on zeolites at certain concentrations similar to metal–organic frameworks known for their flexibility. Kinetically speaking, eq. (44) is valid, just taking into account that the number of molecules in a narrow mesopore should be adjusted considering the expansion factor ξ stemming from the phase transition. More specifically , $n = (\frac{V_{adsorbedspecies}}{V_{pore}})\ \phi\xi$, where $\xi = f(C_A)$. Modelling of such transitions is, however, beyond the scope of the current paper. From the mathematical viewpoint an empirical expression of the enhancement factor ξ can be of the form

$$\xi = 1 + \frac{aC_A{}^l}{1 + bC_A{}^l} \tag{47}$$

where *a, b* and *l* are parameters. Empirical eq. (46) explains a value of the enhancement factor equal to unity at low values of C_A gradually reaching $\xi = 1 + a/b$ upon elevation of the reactant concentration.

The concept presented by eq. (23) can be used not only for large mesopores. The same approach can be also utilized for so-called dendritic zeolites (Alonso-Doncel et al., 2023), exhibiting trimodal porous structure. For ZSM-5 dendritic nanostructures besides the zeolitic micropores of ca. 0.55 nm, also mesopores of the size 3–10 nm with the peak maximum of 5–6 nm along with large mesopores (peak maximum 20 nm) are present. In the context of the current kinetic treatment, the mesopores of ca. 6 nm in diameter are very large in comparison with the cross-section of molecules typically used in catalysis over zeolites. For

example, the cross-section of aromatic compounds, such as those investigated in (Alonso-Doncel et al., 2023), is one order of magnitude lower that the cross-section of the pore, implying that hundreds of molecules can be present within a pore. Subsequently for such type of materials instead of a general expression for the two-step sequence with the second irreversible step

$$r_{s+nm+m} = \frac{(\omega^s_{+1}\omega^s_{+2})}{\omega^s_{+1}+\omega^s_{+2}+\omega^s_{-1}}N^B_s + \frac{(\omega^I_{+1}+\omega^{II}_{+1}U_1+\omega^{III}_{+1}U_1U_2+..+\omega^n_{+1}U_1U_2..U_{n-1})}{1+U_1+U_1U_2+U_1U_2U_3+...+U_1U_2U_3...U_n}N^B_{NM} + \frac{(\omega^M_{+1}\omega^M_{+2})e^{(1-\alpha_2-\alpha_1)\varphi'\sqrt{\rho_{H^+}}}}{\omega^M_{+1}e^{-\alpha_1\varphi'\sqrt{\rho_{H^+}}}+\omega^M_{+2}e^{(1-\alpha_2)\varphi'\sqrt{\rho_{H^+}}}+\omega^M_{-1}e^{(1-\alpha_1)\varphi'\sqrt{\rho_{H^+}}}}N^B_M \quad (48)$$

the reaction rate is simplified

$$r_{s+m} = \frac{(\omega^s_{+1}\omega^s_{+2})}{\omega^s_{+1}+\omega^s_{+2}+\omega^s_{-1}}N^B_s + \frac{(\omega^M_{+1}\omega^M_{+2})e^{(1-\alpha_2-\alpha_1)\varphi'\sqrt{\rho_{H^+}}}}{\omega^M_{+1}e^{-\alpha_1\varphi'\sqrt{\rho_{H^+}}}+\omega^M_{+2}e^{(1-\alpha_2)\varphi'\sqrt{\rho_{H^+}}}+\omega^M_{-1}e^{(1-\alpha_1)\varphi'\sqrt{\rho_{H^+}}}}N^B_M \quad (49)$$

The ratio between the reaction rates over dendritic materials with micropores and relatively large mesopores and zeolites with only micropores bearing a single acid site each can be easily formulated

$$\frac{r_{s+m}}{r_s} = \frac{N^B_{s,dendritic}}{N^B_{s,zeolite}} + \frac{(\omega^M_{+1}\omega^M_{+2})e^{(1-\alpha_2-\alpha_1)\varphi'\sqrt{\rho_{H^+}}}}{\omega^M_{+1}e^{-\alpha_1\varphi'\sqrt{\rho_{H^+}}}+\omega^M_{+2}e^{(1-\alpha_2)\varphi'\sqrt{\rho_{H^+}}}+\omega^M_{-1}e^{(1-\alpha_1)\varphi'\sqrt{\rho_{H^+}}}}\frac{(\omega^s_{+1}+\omega^s_{+2}+\omega^s_{-1})}{\omega^s_{+1}\omega^s_{+2}}\frac{N^B_{M,dendritic}}{N^B_{s,zeolite}} \quad (50)$$

When the isolated acid sites have the same reactivity independent on their location inside a pore or in a large mesopore, the frequency of steps are the same and if the Polanyi parameters are equal for both steps obtaining a typical value of 0.5, one gets instead of eq. (49)

$$\frac{r_{s+m}}{r_s} = \frac{N^B_{s,\,dendritic}}{N^B_{s,\,zeolite}} + \frac{(\omega_{+1}+\omega_{+2}+\omega_{-1})}{\omega_{+1}e^{-\varphi'\sqrt{\rho_{H^+}}}+\omega_{+2}+\omega_{-1})e^{0.5\varphi'\sqrt{\rho_{H^+}}}}\frac{N^B_{M,\,dendritic}}{N^B_{s,\,zeolite}} \quad (51)$$

Eq. (50) is explicitly relating the ratio of rates with the kinetic parameters (the frequencies of steps) and the physico-chemical properties (number of acids sites). Moreover, it contains an implicit dependence on the surface area of the mesoporous materials as

$$\varphi' = \frac{\delta_{Z_{H^+}}N_Ae^2}{4\pi\varepsilon_0\varepsilon}\sqrt{\frac{\pi N_A}{4}}\sqrt{\frac{1}{S_{N_2,mesopores}}} = \psi\sqrt{\frac{1}{S_{N_2,mesopores}}} \quad (52)$$

With

$$\psi = \frac{\delta_{Z_{H^+}}N_Ae^2}{4\pi\varepsilon_0\varepsilon}\sqrt{\frac{\pi N_A}{4}} \quad (53)$$

finally giving an expression containing also the textural properties

$$\frac{r_{s+m}}{r_s} = \frac{N^B_{s,dendritic}}{N^B_{s,zeolite}} + \frac{(\omega_{+1}+\omega_{+2}+\omega_{-1})}{\left(\omega_{+1}e^{-\psi\sqrt{\frac{\rho_{H^+}}{S_{N_2,mesopores}}}}+\omega_{+2}+\omega_{-1}\right)e^{0.5\psi\sqrt{\frac{\rho_{H^+}}{S_{N_2,mesopores}}}}}\frac{N^B_{M,dendritic}}{N^B_{s,zeolite}} \quad (54)$$

For obvious reasons there is a lack of experimental data on catalytic properties of dendritic zeolites with the available limited results not allowing validation of eq. (53). For example, just two values for dendritic ZSM-5 materials are available for LDPE catalytic cracking and one for methane decomposition (Alonso-Doncel et al., 2023). Apparently, this is not sufficient to elucidate applicability of eq. (53) and further research is required.

Many equations above, e.g. eqns. (47) and (48), assume only Brønsted acid sites. Obviously, a more general treatment should include also catalysis on Lewis sites, as generation of mesopores in zeolites may also induce important changes in Lewis acidity. Moreover, formation of mesopores can also influence shape-selectivity, which will be discussed below. The latter concept implies that zeolite catalysts due to the fixed shape and size of the pore structure can function selectively on certain molecules of a particular size and shape. In this sense, chemical reactions occurring over active sites located on the mesopore surface area are expected to take place with no or little shape-selectivity effects.

Eq. (50) assumes that conventional zeolites and their hierarchical counterparts have the same reactivity of an individual acid. In general creation of mesoporosity might result in significant changes in the nature and strength of the acid sites. In particular, dealumination results in removal of aluminium from the framework position and thus lower concentration of Brønsted acid sites, concomitant with an increase of the Lewis acid sites. As the former sites are active in some reactions (e. g. cracking, aromatization, etc) and the latter in e.g. Friedel–Crafts acylation, eq. (49) in a general form should include concentrations of both types of sites and different values of the frequencies of steps making numerical evaluation of the corresponding equation cumbersome without substantial simplifications.

$$(r_{s+m})_{(L+B)dendritic} = \left(\frac{\left(\omega^s_{+1,B,d}\omega^s_{+2,B,d}\right)}{\omega^s_{+1,B,d}+\omega^s_{+2,B,d}+\omega^s_{-1,B,d}}N^B_s + \frac{\left(\omega^s_{+1,L,d}\omega^s_{+2,L,d}\right)}{\omega^s_{+1,L,d}+\omega^s_{+2,L,d}+\omega^s_{-1,L,d}}N^L_s + \frac{\left(\omega^M_{+1,B,d}\omega^M_{+2,B,d}\right)e^{(1-\alpha_2-\alpha_1)\varphi'\sqrt{\rho_{H^+}}}}{\omega^M_{+1,B,d}e^{-\alpha_1\varphi'\sqrt{\rho_{H^+}}}+\omega^M_{+2,B,d}e^{(1-\alpha_2)\varphi'\sqrt{\rho_{H^+}}}+\omega^M_{-1,B,d}e^{(1-\alpha_1)\varphi'\sqrt{\rho_{H^+}}}}N^B_M + \frac{\left(\omega^M_{+1,B,d}\omega^M_{+2,B,d}\right)e^{(1-\alpha_2-\alpha_1)\varphi'\sqrt{\rho_{H^+}}}}{\omega^M_{+1,B,d}e^{-\alpha_1\varphi'\sqrt{\rho_{H^+}}}+\omega^M_{+2,B,d}e^{(1-\alpha_2)\varphi'\sqrt{\rho_{H^+}}}+\omega^M_{-1,B,d}e^{(1-\alpha_1)\varphi'\sqrt{\rho_{H^+}}}}N^L_M \right) \quad (55)$$

4. Shape selectivity

4.1. Microporous materials

Finally, the shape selectivity in microporous materials will be considered focusing on the reactant and product selectivity (Fig. 2).

The classical concepts of shape selectivity in catalysis by zeolites are connected to mass transfer limitations within the pores (Degnan, 2003;

Csicsery, 1984; Weisz and Frilette, 1960) or in particular, configurational diffusion when the size of the intracrystalline pores is in the same range as the size of reacting molecules. The reactant selectivity (Fig. 2) can be thus explained by different values of configurational diffusion coefficients. Another more straightforward explanation is the key-lock concept implying that the geometry at the entrance of the pores can simply prevent more branched reactants from entering a pore.

The product shape selectivity contrary to the reactant shape selectivity means that the reactants of specific orientation cannot diffuse out of the pores. In the case of transition state selectivity (not shown in Fig. 2) steric restrictions of the transition state govern the product distribution.

For the pores of a larger size with several molecules within a narrow mesopore using terminology of the current work, shape selectivity can be related to the loading density of the reactants within the pore (Santilli et al., 1993; Schenk et al., 2002). Moreover, as discussed in (Derouane and Gabelica, 1980; Santilli and Zones, 1990) the secondary shape selectivity can be present because of lateral interactions within the pore influencing the relative rates of diffusion. In terms of kinetic considerations of the present work, such effects can be explained by assuming that geometry of a particular reactant influences the number of such molecules in the pore or the value of n in eq. (25). Moreover, the rate constants for transformations of the reactants can be assumed to depend on the molecules already present inside the pore. Changes in diffusivity or mutual influence within narrow mesopores or on the surface of such mesopores are, however, not sufficient to significantly influence shape selectivity according to Degnan (2003) and Santilli et al. (1993).

The contribution of non-shape selective acid sites at the external surface of the zeolite crystals (Derouane and Gabelica, 1980) should not be neglected as the acid sites on the external surface are located in the cavities formed by the terminus of the pore at the surface and thus can have reactivity and shape selectivity different from the sites within a pore. Even if the external surface area is substantially lower than the area within the pores for conventional zeolites and the acid strength can be also not high. Nevertheless, zeolites can be also synthesised with small crystals (US Patent 5,620,590, 1997) increasing the relative contribution of the external surface area and also reducing the diffusion path of the reactants.

In the treatment below a system with independent reactions A_1->P_1 and A_2->P_2 corresponding to reactant shape selectivity will be discussed. The product shape selectivity on the other hand can be treated from the kinetic viewpoint as just a special case of the reactant shape selectivity.

The reaction rate for the first reaction ($A_1 \rightarrow P_1$) and the second reaction in the system of independent parallel reactions can be described by simplifying eq. (28)

$$r_{A_1\rightarrow P_1} = \gamma_{A_1}(r^B_{A_1\rightarrow P_1,S}N^B_S + r^L_{A_1\rightarrow P_1,S}N^L_S) + r^B_{A_1\rightarrow P_1,C}N^B_C + r^L_{A_1\rightarrow P_1,C}N^L_C \quad (56)$$

$$r_{A_2\rightarrow P_2} = \gamma_{A_2}(r^B_{A_2\rightarrow P_2,S}N^B_S + r^L_{A_2\rightarrow P_2,S}N^L_S) + r^B_{A_2\rightarrow P_2,C}N^B_C + r^L_{A_2\rightarrow P_2,C}N^L_C \quad (57)$$

Where γ_{A_1} and γ_{A_2} are the shape selectivity steric factors for the reactants A_1 and A_2 respectively, which can be of the key-lock or configurational diffusion origin.

To simplify the derivation, only catalysis on Brønsted acid single sites will be considered for the two-step sequence resulting in the following network

	$N^{(A_1\rightarrow P_1)}$	$N^{(A_2\rightarrow P_2)}$
1. *+A_1↔I*	1	0
2. I* ↔* +P_1	1	0
3. *+A_2↔J*	0	1
4. J* ↔* +P_2	0	1
$N^{(A_1\rightarrow P_1)}$: $A_1 \rightarrow P_1$, $N^{(A_2\rightarrow P_2)}$: $A_2 \rightarrow P_2$		

(58)

From the steady state approximation for intermediates I and J

$$k_{+1}C_{A_1}N_0 - k_{-1}N_I = k_{+2}N_I - k_{-2}N_0C_{P_1} \quad (59)$$

$$k_{+3}C_{A_2}N_0 - k_{-3}N_J = k_{+4}N_J - k_{-4}N_0C_{P_2} \quad (60)$$

Where N_I and N_J are surface concentrations of I and J respectively.

One gets in a more general form with the frequencies of steps

$$N_I = \frac{\omega^{B,s}_{+1} + \omega^{B,s}_{-2}}{\omega^{B,s}_{+2} + \omega^{B,s}_{-1}}N_0 = U'_{1,s}N_0 \quad (61)$$

and

$$N_J = \frac{\omega^{B,s}_{+3} + \omega^{B,s}_{-4}}{\omega^{B,s}_{+4} + \omega^{B,s}_{-3}}N_0 = U'_{2,s}N_0 \quad (62)$$

With

$$U'_{1,s} = \frac{\omega^{B,s}_{+1} + \omega^{B,s}_{-2}}{\omega^{B,s}_{+2} + \omega^{B,s}_{-1}}U'_{2,s} = \frac{\omega^{B,s}_{+3} + \omega^{B,s}_{-4}}{\omega^{B,s}_{+4} + \omega^{B,s}_{-3}} \quad (63)$$

Considering the mass balance $N_0 + N_I + N_J = N^B_S$ the expression for the bare sites is

$$N_0 = \frac{N^B_S}{1 + U'_{1,s} + U'_{2,s}} \quad (64)$$

Giving subsequently expressions for the rates along different reaction routes on Brønsted single acid sites

$$r^B_{A_1\rightarrow P_1,S} = \gamma_{A_1}\frac{(\omega^{B,s}_{+2}U'_1 - \omega^{B,s}_{-2})}{1 + U'_{1,s} + U'_{2,s}}N^B_S \quad (65)$$

$$r^B_{A_2\rightarrow P_2,S} = \gamma_{A_2}\frac{(\omega^{B,s}_{+4}U'_1 - \omega^{B,s}_{-4})}{1 + U'_{1,s} + U'_{2,s}}N^B_S \quad (66)$$

In a more general way, the rates on both Brønsted single acid sites and external surfaces would be

$$r_{A_1\rightarrow P_1} = \gamma_{A_1}\frac{(\omega^{B,s}_{+2}U'_{1,s} - \omega^{B,s}_{-2})}{1 + U'_{1,s} + U'_{2,s}}N^B_S + \frac{(\omega^{B,c}_{+2}U'_1 - \omega^{B,c}_{-2})}{1 + U'_{1,c} + U'_{2,c}}N^B_C \quad (67)$$

$$r_{A_2\rightarrow P_2} = \gamma_{A_2}\frac{(\omega^{B,s}_{+4}U'_1 - \omega^{B,s}_{-4})}{1 + U'_{1,s} + U'_{2,s}}N^B_S + \frac{(\omega^{B,c}_{+4}U'_1 - \omega^{B,c}_{-4})}{1 + U'_{1,c} + U'_{2,c}}N^B_C \quad (68)$$

The same approach can be easily expanded to Lewis acid sites.

Simplifications of eqns. (66) and (67) are obviously possible when the second step is irreversible giving

$$r_{A_1\rightarrow P_1} = \gamma_{A_1}\frac{(\omega^{B,s}_{+2}U'_{1,s})}{1 + U'_{1,s} + U'_{2,s}}N^B_S + \frac{(\omega^{B,c}_{+2}U'_1)}{1 + U'_{1,c} + U'_{2,c}}N^B_C \quad (69)$$

$$r_{A_2\rightarrow P_2} = \gamma_{A_2}\frac{(\omega^{B,s}_{+4}U'_1)}{1 + U'_{1,s} + U'_{2,s}}N^B_S + \frac{(\omega^{B,c}_{+4}U'_1)}{1 + U'_{1,c} + U'_{2,c}}N^B_C \quad (70)$$

It is worth to analyse shape selectivity

$$S_{P_1} = \frac{r_{p_1}}{r_{p_1} + r_{p_2}} = \frac{\gamma_{A_1}\frac{(\omega^{B,s}_{+2}U'_{1,s})}{1+U'_{1,s}+U'_{2,s}}N^B_S + \frac{(\omega^{B,c}_{+2}U'_1)}{1+U'_{1,c}+U'_{2,c}}N^B_C}{\gamma_{A_1}\frac{(\omega^{B,s}_{+2}U'_{1,s})}{1+U'_{1,s}+U'_{2,s}}N^B_S + \frac{(\omega^{B,c}_{+2}U'_1)}{1+U'_{1,c}+U'_{2,c}}N^B_C + \gamma_{A_2}\frac{(\omega^{B,s}_{+4}U'_1)}{1+U'_{1,s}+U'_{2,s}}N^B_S + \frac{(\omega^{B,c}_{+4}U'_1)}{1+U'_{1,c}+U'_{2,c}}N^B_C} \quad (71)$$

$$S_{P_1} = \frac{1}{1 + \frac{\gamma_{A_2}\frac{\omega^{B,s}_{+4}U'_1}{1+U'_{1,s}+U'_{2,s}}N^B_S + \frac{\omega^{B,c}_{+4}U'_1}{1+U'_{1,c}+U'_{2,c}}N^B_C}{\gamma_{A_1}\frac{\omega^{B,s}_{+2}U'_{1,s}}{1+U'_{1,s}+U'_{2,s}}N^B_S + \frac{(\omega^{B,c}_{+2}U'_1)}{1+U'_{1,c}+U'_{2,c}}N^B_C}} \quad (72)$$

It follows apparently from eq. (71) that the reactant shape selectivity

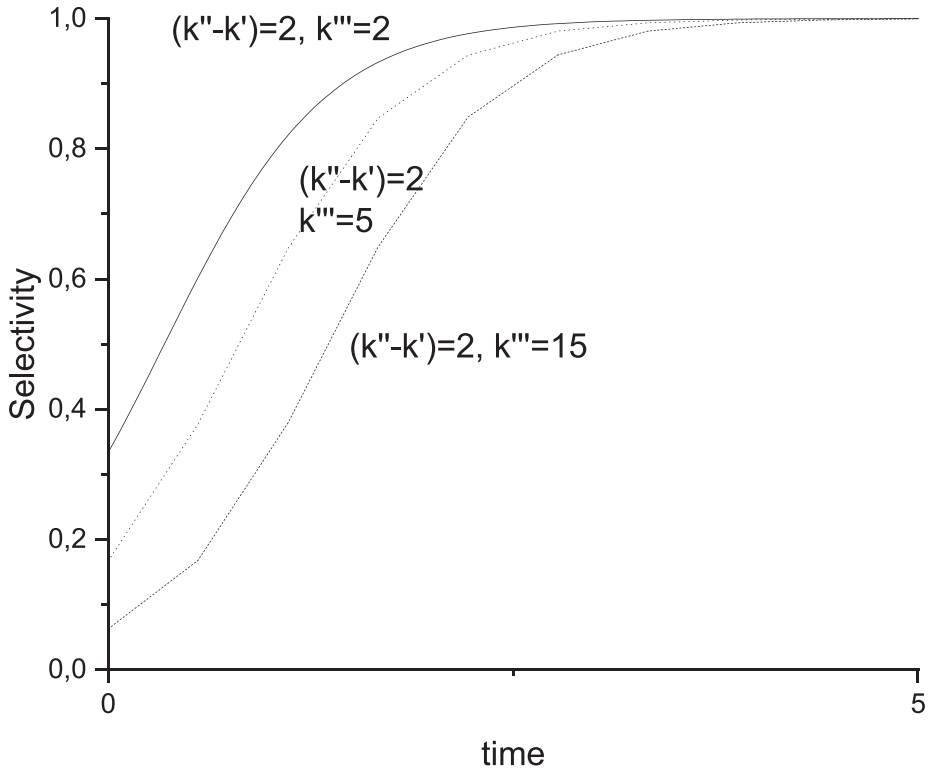

a)

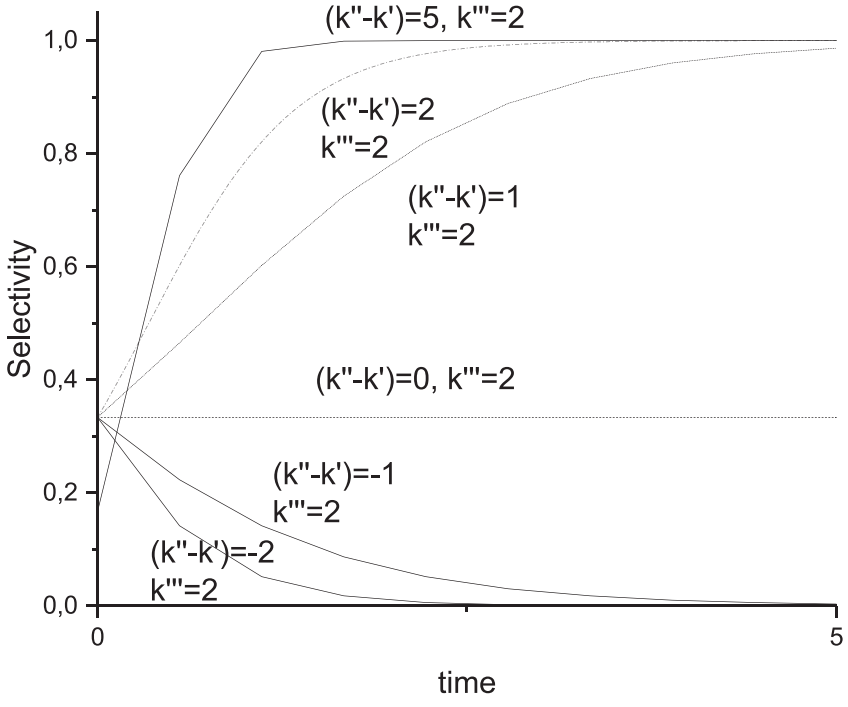

b)

Fig. 3. Numerical analysis of eq. (77) at a) different k''' values, b) at constant k'''=2.

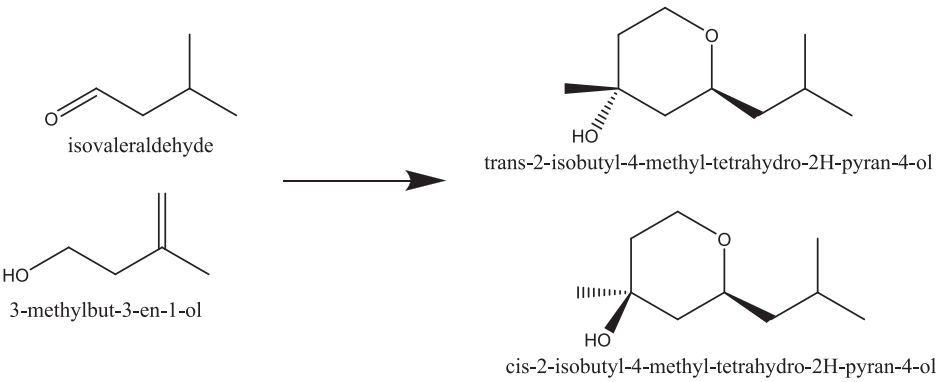

Fig. 4. The scheme of isovaleraldehyde (IVA) condensation with isoprenol (3-methylbut-3-en-1-ol, MOL) giving cis and trans tetrahydropyranol (2-isobutyl-4-methyl-tetrahydro-2H-pyran-4-ol, CisP and TransP, respectively).

depends on the contribution of the reaction on the external surface. When the contribution of the external surface can be neglected eq. (71) is reduced to

$$S_{P_1} = \frac{1}{1 + \frac{\gamma_{A_2} k_{+3}^{B,s} k_{+4}^{B,s} (k_{+2}^{B,s} + k_{-1}^{B,s}) C_{A_2}}{\gamma_{A_1} k_{+1}^{B,s} k_{+2}^{B,s} (k_{+4}^{B,s} + k_{-3}^{B,s}) C_{A_1}}} \tag{73}$$

Apparently, selectivity depends on the ratio between the reactants, rate constants and the shape selectivity steric factors.

An explicit analytical solution for the concentration of reactants is easily available for the first order reactions as the differential equations for the consumption of reactants can be essentially simplified.

$$-\frac{dC_{A_1}}{dt} = \gamma_{A_1} \frac{k_{+2}^{B,s} \frac{k_{+1}^{B,s}}{k_{+2}^{B,s} + k_{-1}^{B,s}} C_{A_1}}{1 + \frac{k_{+1}^{B,s}}{k_{+2}^{B,s} + k_{-1}^{B,s}} C_{A_1} + \frac{k_{+3}^{B,s}}{k_{+4}^{B,s} + k_{-3}^{B,s}} C_{A_2}} N_S^B + \frac{k_{+2}^{B,c} \frac{k_{+1}^{B,c}}{k_{+2}^{B,c} + k_{-1}^{B,c}} C_{A_1}}{1 + \frac{k_{+1}^{B,c}}{k_{+2}^{B,c} + k_{-1}^{B,c}} C_{A_1} + \frac{k_{+3}^{B,c}}{k_{+4}^{B,c} + k_{-3}^{B,c}} C_{A_2}} N_C^B \approx$$

$$\approx \gamma_{A_1} k_{+2}^{B,s} \frac{k_{+1}^{B,s}}{k_{+2}^{B,s} + k_{-1}^{B,s}} C_{A_1} N_S^B + k_{+2}^{B,c} \frac{k_{+1}^{B,c}}{k_{+2}^{B,c} + k_{-1}^{B,c}} C_{A_1} N_C^B = k' C_{A_1} \tag{74}$$

$$-\frac{dC_{A_2}}{dt} = \gamma_{A_2} \frac{k_{+4}^{B,s} \frac{k_{+3}^{B,s}}{k_{+4}^{B,s} + k_{-3}^{B,s}} C_{A_2}}{1 + \frac{k_{+1}^{B,s}}{k_{+2}^{B,s} + k_{-1}^{B,s}} C_{A_1} + \frac{k_{+3}^{B,s}}{k_{+4}^{B,s} + k_{-3}^{B,s}} C_{A_2}} N_S^B + \frac{k_{+4}^{B,c} \frac{k_{+3}^{B,c}}{k_{+4}^{B,c} + k_{-3}^{B,c}} C_{A_2}}{1 + \frac{k_{+1}^{B,c}}{k_{+2}^{B,c} + k_{-1}^{B,c}} C_{A_1} + \frac{k_{+3}^{B,c}}{k_{+4}^{B,c} + k_{-3}^{B,c}} C_{A_2}} N_C^B \approx$$

$$\approx \gamma_{A_2} k_{+4}^{B,s} \frac{k_{+3}^{B,s}}{k_{+4}^{B,s} + k_{-3}^{B,s}} C_{A_2} N_S^B + k_{+4}^{B,c} \frac{k_{+3}^{B,c}}{k_{+4}^{B,c} + k_{-3}^{B,c}} C_{A_2} N_C^B = k'' C_{A_2} \tag{75}$$

With

$$k' = \gamma_{A_1} k_{+2}^{B,s} \frac{k_{+1}^{B,s}}{k_{+2}^{B,s} + k_{-1}^{B,s}} N_S^B + k_{+2}^{B,c} \frac{k_{+1}^{B,c}}{k_{+2}^{B,c} + k_{-1}^{B,c}} N_C^B \tag{76}$$

$$k'' = \gamma_{A_2} k_{+4}^{B,s} \frac{k_{+3}^{B,s}}{k_{+4}^{B,s} + k_{-3}^{B,s}} N_S^B + k_{+4}^{B,c} \frac{k_{+3}^{B,c}}{k_{+4}^{B,c} + k_{-3}^{B,c}} N_C^B \tag{77}$$

Subsequently selectivity behavior in a batch reactor depends on the reaction time as

$$S_{P_1} = \frac{1}{1 + k''' e^{-(k'' - k')t}} \tag{78}$$

With

$$k''' = \frac{\gamma_{A_2} k_{+3}^{B,s} k_{+4}^{B,s} (k_{+2}^{B,s} + k_{-1}^{B,s}) C^0_{A_2}}{\gamma_{A_1} k_{+1}^{B,s} k_{+2}^{B,s} (k_{+4}^{B,s} + k_{-3}^{B,s}) C^0_{A_1}} \tag{79}$$

Fig. 3a featuring numerical analysis of eq. (77) illustrates that for a positive value of $k'' - k' = 2$, the initial selectivity to the product P_1 is increasing for all values of k''' with different initial points. When on the contrary the value of k''' is fixed (Fig. 3b) selectivity can decrease, increase or be constant depending on the value of $(k'' - k')$. The magnitude of the dependence is defined by k''' value.

4.2. Gemini pairs

The treatment above was related to microporous materials with the solution provided for the reactant shape selectivity.

There are experimental data for catalytic reactions on zeolites with mesoporosity indicating that the ratio of products in i.e. aldol condensation of isoprenol with isovaleric aldehyde to cis and trans pyronols (Fig. 4) depends on mesoporosity and the fraction of strong acid sites (Lasne et al., 2022; Shcherban et al., 2022). In (Shcherban et al., 2022) hierarchical beta zeolites with a variable Si/Al ratio, nanoparticle sizes, textural and acidic properties were used to assess the structure–activity relationship.

Due to the mesoporous character of the catalytic materials and the product shape selectivity, it is worth to consider shape selectivity for this

case just using the Gemini pairs for the illustration purpose. In a more general case, there could more acid sites present within a narrow mesopore than just two- Moreover, the treatment below does not include microporosity and pores with a single acid site, however, the derivation can be easily extended to include those sites. For the sake of simplicity the second step in a two-step sequence will be considered as an irreversible one. The reaction mechanism can be represented thus by the following set of reaction routes.

	$N^{(G')cis}$	$N^{(G'')cis}$	$N^{(G')trans}$	$N^{(G'')trans}$
1'.* +IVA↔J*	1	0	1	0
2'. J*+MOL→*+CisP	1	0	0	0
1''.J* + IVA↔J'*	0	1	0	1
2''. J'*+MOL↔J*+CisP	0	1	0	0
3'. J*+MOL→*+TransP	0	0	1	0
4''. J'*+MOL↔J*+TransP	0	0	0	1

$N^{(G')cis}$, $N^{(G'')cis}$: IVA+MOL→CisP; $N^{(G')trans}$, $N^{(G'')trans}$: IVA+MOL→TransP

(80)

In this mechanism it is suggested that because of higher isovaleraldehyde concentration (typical molar excess of 5 (Lasne et al., 2022; Shcherban et al., 2022)) and preferential adsorption of the carbonyl group vs the double bond the first step in the mechanism is binding of isovaleraldehyde. From the steady state approximation

$$k'_{+1,G}C_{IVA}N_{0,G} - k'_{-1,G}N_{J,G} = (k'_{+2,G} + k'_{+3,G})C_{MOL}N_{J,G} \quad (81)$$

$$k''_{+1,G}C_{IVA}N_{J,G} - k''_{-1,G}N_{J',G} = (k''_{+2,G}+k''_{+4,G})C_{MOL}N_{J',G} \quad (82)$$

one gets

$$N_{J,G} = \frac{k'_{+1,G}C_{IVA}}{(k'_{+2,G} + k'_{+3,G})C_{MOL} + k'_{-1,G}}N_{0,G} = U''_1 N_{0,G} \quad (83)$$

$$N_{J',G} = \frac{k'_{+1,G}C_{IVA}}{(k'_{+2,G} + k'_{+3,G})C_{MOL} + k'_{-1,G}}\frac{k''_{+1,G}C_{IVA}}{(k''_{+2,G}+k''_{+4,G})C_{MOL} + k''_{-1,G}}N_{0,G} = U''_1 U''_2 N_{0,G} \quad (84)$$

With

$$U''_1 = \frac{k'_{+1,G}C_{IVA}}{(k'_{+2,G} + k'_{+3,G})C_{MOL} + k'_{-1,G}};\ U''_2 = \frac{k''_{+1,G}C_{IVA}}{(k''_{+2,G}+k''_{+4,G})C_{MOL} + k''_{-1,G}} \quad (85)$$

From the mass balance an expression for the bare sites in the Gemini pair can be obtained

$$N_{0,G} = \frac{N_G}{1 + U''_1 + +U''_1 U''_2} \quad (86)$$

Using eq. (82)–(85) the expressions for the reaction rates of cis- and trans- product formation

$$r_{cis} = (U''_1\omega'_{+2,G} + U''_1 U''_2\omega'_{+3,G})N_{0,G} \quad (87)$$

$$r_{trans} = (U''_1\omega'_{+3,G} + U''_1 U''_2\omega'_{+4,G})N_{0,G} \quad (88)$$

With $N_{0,G}$ defined from eq. (85).

Subsequently, the cis–trans ratio is

$$\frac{r_{cis}}{r_{trans}} = \frac{\left(U''_1\omega'_{+2,G} + U''_1 U''_2\omega'_{+3,G}\right)}{U''_1\omega'_{+3,G} + U''_1 U''_2\omega'_{+4,G}} = \frac{\frac{k'_{+1,G}C_{IVA}k''_{+2,G}C_{MOL}}{(k'_{+2,G}+k'_{+3,G})C_{MOL}+k'_{-1,G}} + \frac{k'_{+1,G}C_{IVA}}{(k'_{+2,G}+k'_{+3,G})C_{MOL}+k'_{-1,G}}\frac{k''_{+1,G}C_{IVA}k'_{+3,G}C_{MOL}}{(k''_{+2,G}+k''_{+4,G})C_{MOL}+k''_{-1,G}}}{\frac{k'_{+1,G}C_{IVA}k'_{+3,G}C_{MOL}}{(k'_{+2,G}+k'_{+3,G})C_{MOL}+k'_{-1,G}} + \frac{k'_{+1,G}C_{IVA}}{(k'_{+2,G}+k'_{+3,G})C_{MOL}+k'_{-1,G}}\frac{k''_{+1,G}C_{IVA}k'_{+4,G}C_{MOL}}{(k''_{+2,G}+k''_{+4,G})C_{MOL}+k''_{-1,G}}} = \quad (89)$$

Or

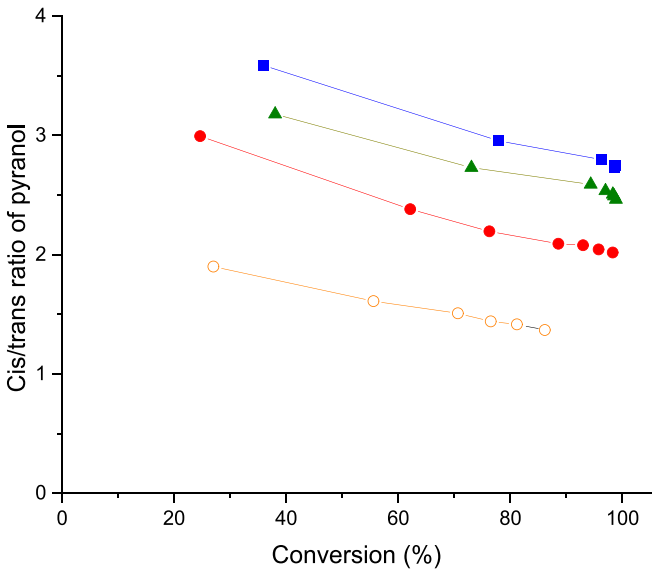

Fig. 5. Cis-trans ratio of pyranols as a function of conversion. Notation: 0.2 M IP and 0.2 M IVA (o), 0.2 M IP and 0.6 M IVA (●), 0.2 M IP and 1.0 M IVA (▲) and 0.2 M IP and 1.4 M IVA (■) molar ratio of isoprenol to isovaleraldehyde.

$$\frac{r_{cis}}{r_{trans}} = \frac{k'_{+1,G}C_{IVA}k''_{+2,G}C_{MOL} + \frac{k''_{+1,G}C_{IVA}k'_{+1,G}C_{IVA}k'_{+3,G}C_{MOL}((k'_{+2,G}+k'_{+3,G})C_{MOL}+k'_{-1,G})}{(k''_{+2,G}+k''_{+4,G})C_{MOL}+k''_{-1,G}}}{k'_{+1,G}C_{IVA}k'_{+3,G}C_{MOL} + \frac{k''_{+1,G}C_{IVA}k'_{+4,G}C_{MOL}k'_{+1,G}C_{IVA}}{(k''_{+2,G}+k''_{+4,G})C_{MOL}+k''_{-1,G}}} \quad (90)$$

When the molar concentration of isoprenol (3-methylbut-3-en-1-ol, MOL) is fixed eq. (89) is modified to a very simple one

$$\frac{r_{cis}}{r_{trans}} = \frac{1 + p_1 C_{IVA}}{p_2 + p_3 C_{IVA}} \quad (91)$$

With

$$p_1 = \frac{k''_{+1,G}k'_{+1,G}k'_{+3,G}((k'_{+2,G} + k'_{+3,G})C_{MOL} + k'_{-1,G})}{(k'_{+1,G}k''_{+2,G})((k''_{+2,G}+k''_{+4,G})C_{MOL} + k''_{-1,G})};\ p_2 = \frac{k'_{+1,G}k'_{+3,G}}{k'_{+1,G}k''_{+2,G}};\ p_3 = \frac{k''_{+1,G}k'_{+4,G}k'_{+1,G}}{k'_{+1,G}k''_{+2,G}((k''_{+2,G}+k''_{+4,G})C_{MOL} + k''_{-1,G})} \quad (92)$$

illustrating that the cis/trans ratio is higher at higher concentrations of isovaleraldehyde when $p_2 \ll p_3 C_{IVA}$ in line with experimental data of Shcherban et al. (2022). When an increase of the excess of isovaleraldehyde the cis/trans ratio is less sensitive, approaching a plateau, also in line with the experiments (Fig. 5). The cis/trans ratio changes with conversion, because of the consecutive dehydration reactions of pyranols, which are more prominent for the *cis*-isomer.

5. Conclusions

An approach to kinetics on zeolitic materials containing different types of pores and acid sites has been developed considering sites on the external surface, isolated single sites, narrow mesopores with few sites and large pores with the acid site density as a descriptor for the latter case. The two-step sequence was considered on both Bronsted and Lewis acid sites.

General rate equations have been derived and analyzed from the viewpoint of the number of acid sites in narrow mesopores.

Potential changes in reactivity are quantitatively considered for materials where mesopores are created upon desilication or dealumination. It was demonstrated that the ratio of rates before and after such treatment depends on the number of acid sites in mesopores and

also on the rate parameters on the second site in a pore with two sites. Large attractive interactions elevating these values will lead to the rate enhancement.

Analysis of the reaction order in materials exhibiting mesoporosity showed that the reaction order in the substrate can exhibit a rather rich behavior, especially compared to the reaction on single sites. Depending on the values of the rate and adsorption constants, different behavior can be expected for the forward rate including the second order in the reactant or even a maximum in the rate upon an increase in the reactant concentration.

A phenomenological enhancement factor was introduced accounting for flexibility of the zeolite framework expanding the pores upon elevation of the reactant concentration.

Kinetic analysis was extended for the special case of dendritic zeolites illustrating in a quantitative way the ratio between the reaction rates over dendritic materials with micropores and relatively large mesopores and zeolites with only micropores bearing a single acid site. Such ratio depends on the kinetic parameters (the frequencies of steps), the physico-chemical properties such as the number of acids sites and the surface area of the mesoporous materials. Analysis of shape selectivity in microporous materials was done for product and reactant shape selectivity deriving the generic rate equations and including explicitly contribution of non-shape selective acid sites at the external surface of the zeolite crystals.

Dependence of product shape selectivity for zeolites exhibiting mesoporosity was illustrated for aldol condensation of isoprenol with isovaleric aldehyde resulting in cis and trans pyronols.

CRediT authorship contribution statement

Dmitry Yu. Murzin: Writing – original draft, Methodology, Formal analysis, Conceptualization.

Declaration of competing interest

The authors declare that they have no known competing financial interests or personal relationships that could have appeared to influence the work reported in this paper.

Data availability

Data will be made available on request.

References

Alonso-Doncel, M., Ochoa-Hernández, C., Gómez-Pozuelo, G., Oliveira, A., González-Aguilar, J., Peral, Á., Sanz, R., Serrano, D.P., 2023. Dendritic nanoarchitecture imparts ZSM-5 zeolite with enhanced adsorption and catalytic performance in energy applications. J. Energy Chem. 80, 77–88.

Arsenova-Härtel, N., Bludau, H., Haag, W.O., Karge, H.G., 2000. Influence of the zeolite pore structure on the kinetics of disproportionation of ethylbenzene. Microp. Mesop. Mater. 25–36, 113–119.

Barakov, R., Shcherban, N., Mäki-Arvela, P., Yaremov, P., Bezverkhyy, I., Wärnå, J., Murzin, D.Y., 2022. Hierarchical beta zeolites as catalysts in α-pinene oxide isomerization. ACS Sust. Chem. Eng. 10, 6642–6656.

Boronat, M., Corma, A., 2019. What is measured when measuring acidity in zeolites with probe molecules? ACS Catal. 9, 1539–1548.

Cejka, J., Corma, A., Zones, S., 2010. Zeolites and Catalysis: Synthesis, Reactions, and Applications. Wiley-VCH, Weinheim, Germany.

Corma, A., Li, C., Moliner, M., 2018. Building zeolites from pre-crystallized units: Nanoscale architecture. Ang. Chem. Int. Ed. 57, 15330–15353.

Csicsery, S.M., 1984. Shape-selective catalysis in zeolites. Zeolites 4, 202–213.

Damjanovic, L., Auroux, A., 2008. Handbook of Thermal Analysis and Calorimetry; Recent Advances, Techniques and Applications; Brown, M.E., Gallagher, P.K., Eds.; Elsevier: Amsterdam, The Netherlands, Volume 5.

Degnan, T.F., 2003. The implications of the fundamentals of shape selectivity for the development of catalysts for the petroleum and petrochemical industries. J. Catal. 216, 32–46.

Derouane, E.G., Gabelica, Z., 1980. A novel effect of shape selectivity: molecular traffic control in zeolite ZSM-5. J. Catal. 65, 486.

Derouane, E.G., Védrine, J.C., Pinto, R.R., Borges, P.M., Costa, L., Lemos, L., Ribeiro, F. R., 2013. The acidity of zeolites: Concepts, measurements and relation to catalysis: a review on experimental and theoretical methods for the study of zeolite acidity. Cat. Rev. 55, 454–515.

Dib, E., Grand, J., Gedeon, A., Mintova, S., Fernandez, C., 2021. Control the position of framework defects in zeolites by changing the symmetry of organic structure directing agents. Microp. Mesop. Mater. 315, 110899.

Fogler, H.S., 2016. The Elements of Chemical Reaction Engineering, 5th ed. Prentice Hall, Hoboken, NJ, USA, p. 992.

Ghojavand, S., Dib, E., Mintova, S., 2023. Flexibility in zeolites: origin, limits and evaluation. Chem. Sci. 14, 12430–12446.

Horiuti, J., Nakamura, T., 1967. On the theory of heterogeneous catalysis. Adv. Catal. 17, 1–74.

Jess, A., Wasserschied, P., 2013. Chemical Technology. Wiley-VCH, Weinheim, Germany.

Kubicka, D., Kumar, N., Venäläinen, T., Karhu, H., Kubickova, I., Österholm, H., Murzin, D.Y., 2006. The metal-support interactions in zeolite-supported noble metals: The influence of metal crystallites on the support acidity. J. Phys. Chem. B 110, 4937–4946.

Laidler, K.J., 1987. Chemical Kinetics, 3rd ed. London, UK, Pearson.

Laluc, M., Barakov, R., Mäki-Arvela, P., Shcherban, N., Murzin, D.Y., 2021. Catalytic activity of hierarchical beta zeolites in the Prins cyclization of (−)-isopulegol with acetone. Appl. Cat. A Gen. 618, 118131.

Langmuir, I., 1922. Part II. Heterogeneous reactions. Chemical reactions on surfaces. Trans. Faraday Soc. 17, 607–620.

Lasne, B., Mäki-Arvela, P., Aho, A., Vajglova, Z., Eränen, K., Kumar, N., Sanchez-Velandia, J., Peurla, M., Mondelli, C., Perez-Ramirez, J., Murzin, D.Y., 2022. Synthesis of Florol via Prins cyclisation over heterogeneous catalysts. J. Catal. 405, 288–302.

Li, C., Ferri, P., Paris, C., Moliner, M., Boronat, M., Corma, A., 2021. Design and synthesis of the active site environment in zeolite catalysts for selectively manipulating mechanistic pathways. J. Am. Chem. Soc. 143, 10718–10726.

Masel, R.J., 2011. Chemical Kinetis and Catalysis. Wiley, Weinheim, Germany.

Milakovic, L., Hintermeier, P.H., Liu, Y., Barath, E., Lercher, J.A., 2021. Influence of intracrystalline ionic strength in MFI zeolites on aqueous phase dehydration of methylcyclohexanols. Ang. Chem. Int. Ed. 60, 24806–24810.

Murzin, D.Y., 2022a. Acid density as a kinetic descriptor of catalytic reactions over zeolites. Chemistry 4, 1609–1623.

Murzin, D.Y., 2022b. Cooperative catalytic nanokinetics. Chem. Eng. Sci. 256, 117684.

Murzin, D.Y., 2022c. Kinetics of two-step catalytic sequence on nanoclusters with limited cluster occupancy. Chem. Eng. J. 450, 138178.

Murzin, D.Y., 2022d. Chemical Reaction Technology. de Gruyter, Berlin, Germany.

Murzin, D.Y., 2023. Kinetics of heterogeneous single-site catalysis. ChemCatChem 15, e202201082.

Murzin, D.Y., Salmi, T., 2016. Catalytic Kinetics, Chemistry and Engineering, 2d ed. Elsevier.

US Patent 5,620,590, 1997, [assigned to Mobil Oil], April 15.

Qi, L., Li, J., Wei, Y., He, Y., Xu, L., Liu, Z., 2016. Influence of acid site density on the three-staged MTH induction reaction over HZSM-5 zeolite. RSC Adv. 6, 52284–52291.

Santilli, D.S., Harris, T.V., Zones, S.I., 1993. Inverse shape selectivity in molecular sieves: Observations, modelling, and predictions. Micropor. Mater. 1, 329.

Santilli, D.S., Zones, S.I., 1990. Secondary shape selectivity in zeolite catalysis. Catal. Lett. 7, 383.

Schenk, M., Calero, S., Maesen, T.L.M., van Benthem, L.L., Verbeek, M.G., Smit, B., 2002. Understanding zeolite catalysis: Inverse shape selectivity revisited. Angew. Chem. Int. Ed. 41, 2500.

Shamzhy, M., Gil, B., Opanasenko, M., Roth, W.J., Cejka, J., 2021. MWW and MFI frameworks as model layered zeolites: structures, transformations, properties and activity. ACS Catal. 11, 2366–2396.

Shcherban, N., Barakov, R., Lasne, B., Mäki-Arvela, P., Shamzhy, M., Bezverkhyy, I., Wärnå, J., Murzin, D.Y., 2022. Florol synthesis via Prins cyclization over hierarchical beta zeolites. Molec. Catal. 531, 112683.

Suib, S.L., Prech, J., Szaniawska, E., Cejka, J., 2023. Recent advances in tetra- (Ti, Sn, Zr, Hf) and pentavalent (Nb, V, Ta) metal-substituted molecular sieve catalysts. Chem. Rev. 123, 877–917.

Temkin, M.I., 1979. The kinetics of some industrial heterogeneous catalytic reactions. Adv. Catal. 28, 173–291.

Weisz, P.B., Frilette, V.J., 1960. Intracrystalline and molecular-shape-selective catalysis by zeolite salts. J. Phys. Chem. 64, 382.

Zhang, Q., Yu, J., Corma, A., 2020. Applications of zeolites to C1 chemistry: Recent advances, challenges, and opportunities. Adv. Mat. 32, 2002927.